Compliant Bistable Gripper for Aerial Parching and Crasning

Haijie Zhang, Jiefeng Sui

Abstract-Small aerial robots usually face a common challenge: they can only fly for a short time due to their limited onboard energy supply. To tackle this issue, one promising solution is to endow flying robots with perching capability so that they can perch or land on walls, trees, or power lines to rest or recharge. Such perching capability is especially useful for monitoring-related tasks since the robot can maintain a desired height for monitoring without flying. One of the major challenges for perching is to design a light-weight and energyefficient perching mechanism. In this paper, we present a 3Dprinted compliant bistable gripper which is easy to close, stable to hold, and easy to adjust for a palm-size quadcopter to perch on cylindrical objects. If installed on the bottom of aerial robots, it can also be used for aerial grasping. The gripper can be directly activated by the impact force during contact to switch from open state to closed state. It can also hold the quadcopter safely since the required force to open the gripper is larger than the robot weight. We analyze the required forces for closing and opening to provide design guidelines for the mechanism. Experimental results show that the designed gripper can successful make the quadcopter perch on cylinders as well as grasp objects.

### I. INTRODUCTION

Aerial robots with multiple rotors (e.g., quadcopters) are widely used in various civilian and military situations such as rescue, surveillance, and monitoring, etc. However, multi-rotor based aerial robots face a critical bottleneck: limited flight time. In fact, the flight time for commercial quadcopters is usually less than one hour due to the low aerodynamic efficiency and high energy consumption [1]. The time is even much shorter for small quadcopters in centimeter scales. For example, the Crazyflie from Bitcraze can only fly for less than 10 minutes. One possible solution is to let aerial robots land or perch on an object (e.g., trees, power lines, or roof) so that they can save and even harvest energy instead of hovering in the air [2], [3]; meanwhile, they can still monitor or surveil an interested area. However, successful perching for aerial robots is challenging since it involves several important parts including mechanical perching mechanism design, flight state estimation, motion planning and control [2].

In our previous research, we have investigated the estimation and control aspect by leveraging visual information to estimate the flight states and control the contact velocity between the aerial robots and the perching object [4], [5].

\*This work is partially supported by the National Science Foundation under Grant IIS-1815476.

<sup>1</sup>Haijie Zhang, Jiefeng Sun, and Jianguo Zhao are with Department of Mechanical Col-Engineering, CO 80523. USA. orado State University, Fort Collins, zhanghaijason@gmail.com, J.Sun@colostate.edu, Jianguo.Zhao@colostate.edu

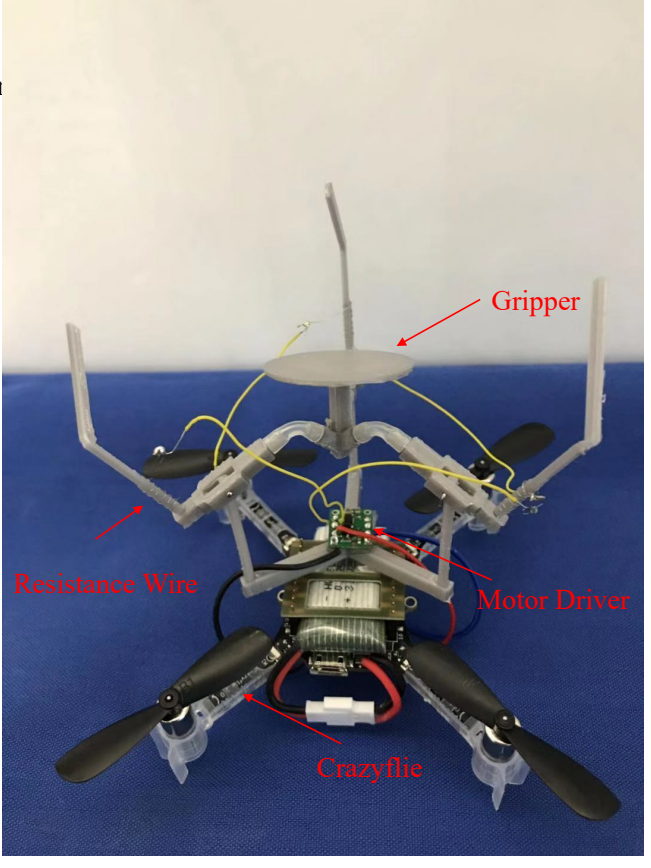


Fig. 1. Perching system. The bistable gripper is installed on the Crazyflie with open state. The Crazyflie can close the gripper and perch on horizontally hanged object. The motor driver and resistance wire are used to release Crazyflie from perching

In addition to the estimation and control aspect, mechanical mechanisms are also critical for successful perching. Ideally, the mechanism should be able to absorb the landing impact, firmly attach to or grasp a desired perching object, and require minimal efforts for releasing. In this paper, we aim to investigate a novel perching mechanism for small quadcopters, which will be ultimately integrated with our estimation, planning, and control algorithms to enable vision-guided autonomous perching.

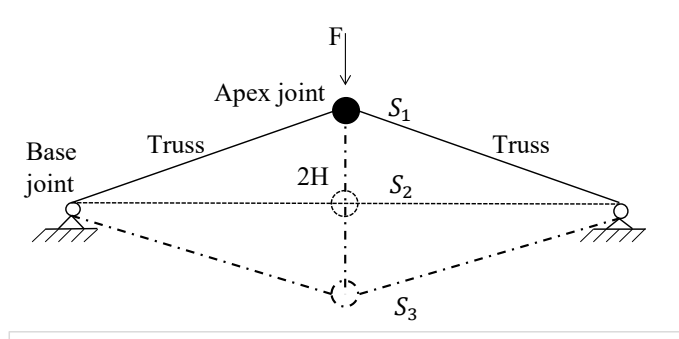
Many researchers have investigated perching mechanism design recently. Graule *et al.* leverage switchable electrostatic adhesion to make the Robobee perch on various objects such as glass, wood, and a natural leaf [6]. Kovač *et al.* design a 4.6 g perching mechanism to convert the landing impact into a snapping movement that inserts a needle into natural or artificial perching object [7]. Inspired by birds, Mehanovic *et al.* adopt a thrust-assisted pitch-up motion to decrease the forward speed of a fixed-wing drone. Combined with microspines, this design allows the drone to perch and take off safely with onboard sensors [8]. Thomas *et al.* develop a gecko-inspired adhesive gripper for both perching

on smooth surface and carrying payloads [9]. With a tail-based mechanism, Stanford Climbing and Aerial Maneuvering Platform (SCAMP) can fly, perch onto outdoor surfaces, climb, and take off again [10]. In [11], researchers transfer a quadcopter's weight into tendon tension and passively actuate the gripping foot. A thorough review for perching can be found in [2].

Another promising type of mechanisms that can be used for perching is bistable mechanisms, which can stay at two stable states without power input and can change from one state to another with an activation force [12]. Thus, it is ideal for a perching since only an activation force is needed to trigger the state change. Since we will design a bistable gripper for perching, we briefly review existing research on bistable mechanisms. Nguyen et al. designed a bistable gripper to carry payloads [13]. Chen et al. used multi-material 3D printing to design a bistable structure [14]. With tunable activation forces, the base bistable structure could be connected serially. Later, they utilized the basic bistable structure and shape memory alloy to actuate an untethered, soft swimming robot [15]. Algasimi et al. presented a new linear bistable compliant crank-slider mechanism [16]. With a pseudo-rigidbody model, they derive the kinetic and kinematic equations to provide a step-by-step design guideline. To better model the force-displacement relationship of bistable mechanism, Li et al. proposed a tri-root bistable function [17]. Qiu et al. also used two curved centrally-clamped parallel beams to design a bistable mechanism [18]. Despite the above research, bistable or multistable mechanism has been widely used for energy- and motion-related applications including morphing features, self-locking structures, energy harvesters and sensors for micro-electromechanical systems [19].

In this paper, we aim to investigate a miniature bistable mechanism for perching and grasping purposes. The whole perching system is shown in Fig. 1. The bistable gripper is installed on top of Crazyflie for perching. Motor driver and resistance wires are used for taking-off. The contributions for this paper are two-fold. First, the bistable mechanism is unique that we leverage low-cost 3D printing for the rigid parts and commercially available soft silicone tubes for the compliant joints. Such a design allows us to rapidly and economically explore different sizes and characteristics for the mechanisms because of 3D-printing and many choices associated with silicone tubes [20]. Second, we establish mathematical models for the mechanism to characterize the activation forces. Based on such models, we also formulate a basic design guideline to achieve desired activation forces under different requirements from perching or grasping.

The rest of this paper is organized as follows. Section II describes the overall concept and the mechanical design of the bistable gripper. Section III presents the mathematical model of the force-displacement relationship of the bistable mechanism. Then we discuss the fabrication and experiments for the mechanism in section IV. We also verify the analytical models with experiments and demonstrate successful perching and taking off using a palm-size quadcopter equipped with the designed bistable gripper.



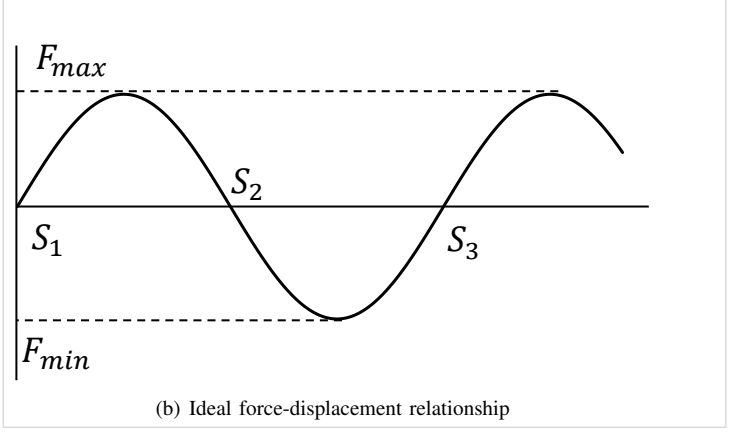


Fig. 2. Basic VMT mechanism and ideal force-displacement relationship. The force-displacement relationship for an ideal VMT is symmetric,  $F_{max} = -F_{min}$ . Stable states are  $S_1$  and  $S_3$ , while  $S_2$  is an unstable state.

### II. DESIGN OF THE BISTABLE GRIPPER

Our proposed bistable gripper is based on Von Mises Truss (VMT) [21] which utilizes the buckling behavior of a truss to change stable states. The basic VMT structure and ideal force-displacement relationship is shown in Fig. 2. Two identical straight trusses are connected with an apex revolute joint. The other end of the trusses are connected to a base revolute joint, respectively. With a vertically applied force F, the apex joint will go downward as the two trusses buckle. If the force is larger than the maximum force  $F_{max}$  in Fig. 2(b), the apex joint can go from stable state  $S_1$  to another stable state  $S_3$  through the unstable state  $S_2$ . The two extreme forces  $F_{max}$ ,  $F_{min}$  are the activation forces which can change the VMT' stable states. For an ideal VMT, the force-displacement relationship is symmetric about horizontal axis, meaning  $F_{max} = -F_{min}$ .

Based on VMT, we aim to design a gripper with bistable states, which can be used both for perching on and grasping objects. To design this gripper, we need to meet several requirements: 1) Easy to close: the activation force at open state ( $F_{max}$ ) should be small enough for small aerial robots to exert. 2) Stable to hold: the activation force at closed state ( $F_{min}$ ) should be large enough to hold the weight of aerial robots during perching or hold weight of payloads during grasping. 3) Easy to adjust: the gripper should be easily adjusted for aerial robots or payloads with different weights.

To meet the three requirements, we need to generate asymmetric force-displacement relationship with different magnitudes for  $F_{max}$  and  $F_{min}$ . Towards this goal, we design

our bistable mechanism as shown in Fig. consists of four main parts: a base with sets of fingers (upper and lower), three sil contact pad with three handles. One end o are connected to the three base beams v joints. The other ends of the fingers are handles on the contact pad with tubes. If applied, the contact pad and fingers will n of their larger dimensions. But the three base with tubes will be bent to switch from another. At the bottom stable state, the upp to hold the payload or quadcopter as long the payload or quadcopter is lighter than the

The proposed design can meet the thr ments. First, the soft silicone tubes serjoints can generate an asymmetric forcetionship. At the bottom stable state, the tubat the top stable state, the tube is bent v stored in it, requiring a smaller activation

can design different bases with different times angles for the three beams. A proper tilted angle can be chosen to adjust the amplitude of the activation forces (both  $F_{max}$  and  $F_{min}$ ) without changing the other parts.

When perching, as long as the quadcopter can provide enough upward thrust, the gripper can close and hold the quadcopter. Moreover, with a properly designed  $F_{max}$ , the gripper will always be closed and hold the quadcopter. To open the gripper after it is closed, there are two possible methods. First, we can generate a downward thrust for the quadcopter. If the thrust force together with the weight is larger than  $F_{max}$ , the gripper can be opened. Second, we can also design a releasing mechanism. A simple design will be wrapping some resistance wires around the upper fingers. Since the fingers will be printed with a thermoplastic material, heating up the resistance wire will soften the beam to open the gripper.

#### III. MATHEMATICAL MODELING

Successful transitions between stable states rely on activation forces  $(F_{max}, F_{min})$ , which can be calculated from the force-displacement relationship of the bistable mechanism. To analyze the mechanism, we detail one branch of the mechanism at two configurations in Fig. 4. The initial stable configuration is plotted on the left half, while the other stable configuration is shown on the right half. We neglect the upper fingers since they do not influence the modeling of forces. The activation forces will depend on many parameters such as the length and Young's modulus of the beam, the length and Young's modulus of the tube, as well as two geometrical parameters: 1) the tilted angle  $\alpha$  for the beam with respect to the vertical line, 2) the tilted angle  $\beta$  for the three handles on the contact pad to the horizontal direction. Both  $\alpha$  and  $\beta$  will influence the force-displacement relationship. To simplify the analysis, however, we will assume a constant  $\beta = \beta_0$ .  $\beta_0$  is selected as when  $\alpha = 0$  and the tube is straight (i.e., no elastic energy is stored in the tube) at the bottom stable state.

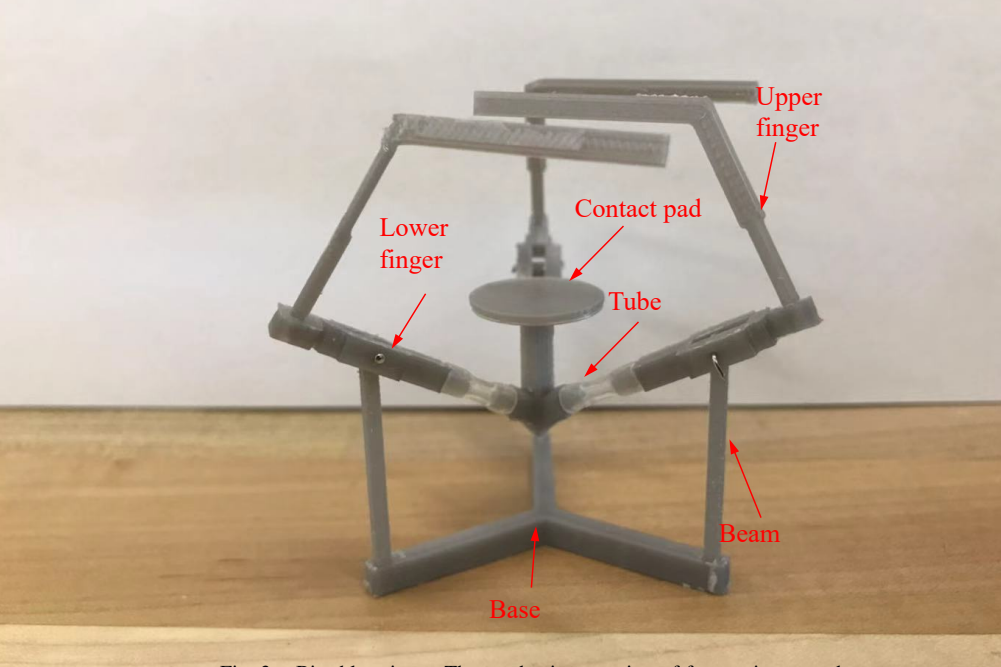


Fig. 3. Bistable gripper. The mechanism consists of four main parts: three fingers (upper and lower), three soft silicone tubes, a base with three vertical beams, and a contact pad.

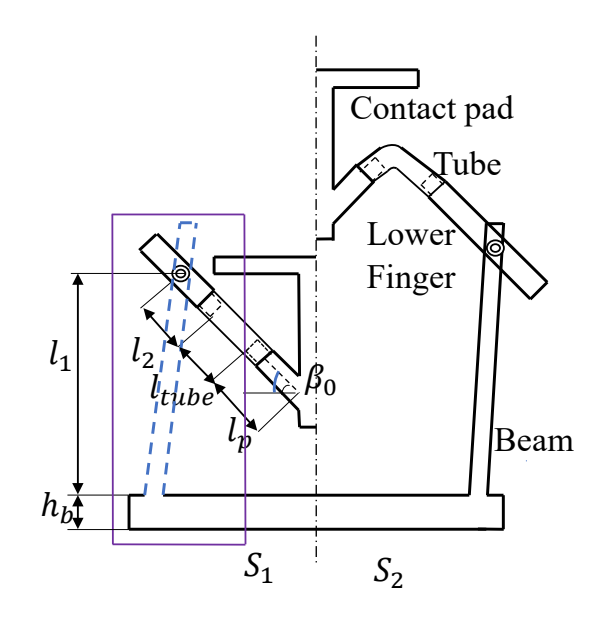


Fig. 4. Two stable states of the proposed mechanism. The left part is the initial designed state  $S_1$ , while the right part is the second stable state  $S_2$ .

To derive the force-displacement relationship, we take out the purple part in Fig. 4 and redraw it in Fig. 5, where  $C_1$  is the initial stable configuration and  $C_2$  is another configuration after we apply a vertical upward force f. In the analysis, we model the base beam as a linear spring with a spring constant  $k_d$ , and the tube as a torsion spring with spring constant  $k_\theta$ . Note that with  $\alpha \neq 0$  and our choice of  $\beta_0$ , there is elastic energy stored in the tube at  $C_1$ .

Assume the beam bending angles are small enough, we can have two resulting assumptions: 1) the vertical distance from the revolute joint to the base is always the same  $l_1$ ; 2) The beam is not bent in  $C_1$  configuration. The other

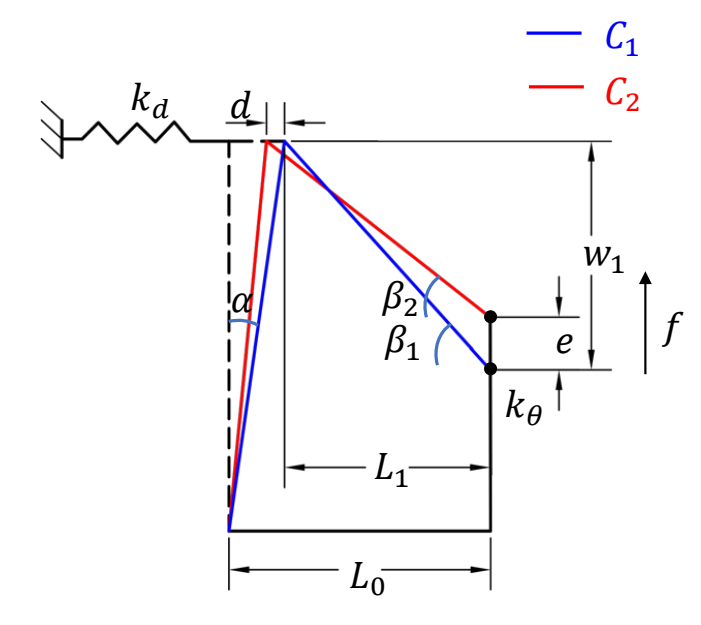


Fig. 5. Schematic for analytic modeling of the bistable mechanism. The beam is modeled as a linear spring with spring constant  $k_d$ , while the tube is treated as a torsion spring with spring constant  $k_{\theta}$ . Ideally, the torsion spring can only move in vertical direction.

parameters are defined as follows:  $L_0$  is the horizontal distance from the tube center to the beam, which can be calculated from  $L_0 = l_3 \cos \beta_0$ , where  $l_3 = (l_2 + l_{tube}/2)$  is the distance from tube center to the revolute joint when  $\alpha = 0$  ( $l_2$  and  $l_{tube}$  are labeled in Fig. 4).

The force-displacement relationship can be obtained by analyzing the movement from the stable state  $C_1$  to another configuration  $C_2$  under an upward force f. Assume the vertical distance from tube center to the linear spring is  $w_1$  and the angle between bottom finger and horizontal dashed line is  $\beta_1$ . When f is applied,  $C_2$  is achieved. The tube is moved upward by e, which is the displacement of the contact pad. Also, the beam is pushed toward left by d, and the finger rotates to a new position with an angle  $\beta_2$  with respect to the horizontal line.

With these parameters, the force-displacement relationship can be derived from principle of minimum potential energy (MPE) [22]. MPE shows that the total potential energy  $E_t$  of a conservative structural system contains both the elastic strain energy  $E_e$ , which is stored in the deformed structure, and the work potential  $E_w$  done by applied force.

$$E_t = E_e + E_w \tag{1}$$

For moving the mechanism from  $C_1$  to  $C_2$ , the equation can be rewritten as

$$E_{t} = \frac{1}{2}k_{d}d^{2} + \frac{1}{2}k_{\theta}\Delta\beta_{2}^{2} - \frac{1}{2}k_{\theta}\Delta\beta_{1}^{2} - fe$$

$$= \frac{1}{2}k_{d}d^{2} + \frac{1}{2}k_{\theta}(\beta_{2} - \beta_{0})^{2} - \frac{1}{2}k_{\theta}(\beta_{1} - \beta_{0})^{2} - fe$$
(2)

In Fig. 5, the geometrical relationship shows:

$$\begin{cases} w_1^2 + L_1^2 = (w_1 - e)^2 + (L_1 + d)^2 \\ \beta_1 = \arctan \frac{w_1}{L_1} \\ \beta_2 = \arctan \frac{w_1 - e}{L_1 + d} \end{cases}$$
 (3)

where

$$\begin{cases} L_1 = L_0 - l_1 \sin \alpha = l_3 \cos \beta_0 - l_1 \sin \alpha \\ w_1 = \sqrt{l_3^2 - L_1^2} = \sqrt{l_3^2 - (l_3 \cos \beta_0 - l_1 \sin \alpha)^2} \end{cases}$$
(4)

The MPE also indicates the extremum of  $E_t$  is where the system will be stable. Thus, we can find the stable configurations by setting  $\frac{\partial E_t}{\partial e} = 0$  to finally obtain the force-displacement function:

$$F(e) = -\frac{3}{L_{f1}} \left[ k_d (L_1 - L_{f1}) (w_1 - e) + k_\theta \left( \arctan\left(\frac{w_1 - e}{L_{f1}}\right) - \beta_0 \right) \right]$$
(5)

where  $L_{f1} = \sqrt{2w_1e + L_1^2 - e^2} = L_1 + d$ .

Among these parameters,  $l_1$ ,  $l_3$ ,  $\beta_0$ ,  $k_d$ ,  $k_\theta$  and  $\alpha$  can be predefined, and e is the displacement variable. When e=0,  $L_1=L_{f1}$ , thus there is no compression for the linear spring (no bending for the beams). And if  $\beta_0 > \beta_1$ , it means a downward force is generated from the tubes. This phenomenon can be explained with our previous assumption that at  $C_1$ , the beams are not bent but the tubes are bent a little bit.

### A. Design guideline for the bistable mechanism

As discussed earlier, the bistable gripper should satisfy three requirements: easy to close, stable to hold, and easy to adjust. By simulating the force-displacement relationship, we find that  $k_{\theta}$  values can change the asymmetry effectively and influence the activation forces accordingly, while  $k_d$  only affects the amplitude of activation forces. With appropriate combinations of  $k_d$  and  $k_{\theta}$ , a small activation force to close the finger and a large activation force to open the finger can be found. With the tilted beams (i.e.,  $\alpha \neq 0$ ), a bistable gripper with one contact pad but with different bases can be designed to satisfy the requirements.

However, without a design method, we can only try different  $k_d$  and  $k_\theta$  and check whether the resulting activation forces are desirable or not. To design a gripper with specific activation forces, we propose a design guideline as follows. For the force-displacement relationship equation F(e), if the mechanism is bistable, F(e) should have two extremes. Thus, we have

$$\begin{cases}
F(e_1) = F_{max} \\
F(e_2) = F_{min} \\
F'(e_1) = 0 \\
F'(e_2) = 0
\end{cases}$$
(6)

where  $e_1$  and  $e_2$  are the displacements corresponding to the two stable configurations. If we want to find the appropriate  $k_d$  and  $k_\theta$  to achieve the desired activation forces, we have 4 unknowns  $e_1$ ,  $e_2$ ,  $k_d$  and  $k_\theta$  and 4 equations. Thus, the

four unknowns can be solved. Similarly, if  $k_d$  and  $k_\theta$  are predefined, we can choose the mechanism dimensions (i.e.,  $l_1$ ,  $l_2$ , and  $\alpha$ ) so that the desired activation forces can be achieved.

In our work, we set  $k_d$  and  $k_{\theta}$  as design variables and predefine the other parameters. With the solved  $k_d$  and  $k_{\theta}$ , we can further calculate the dimension of the beams and tubes to achieve the desired activation forces.

### IV. EXPERIMENTAL RESULTS

In this section, we detail the fabrication of the gripper, setup of experiments, and the results to show that the proposed bistable gripper can be used for perching of flying robot. First, we present the fabrication of three different grippers. After that, we experimentally measure the activation forces to compare with the mathematical results. Finally, we demonstrate the perching by putting the gripper onto a palm-size quadcopter: Crazyflie 2.0 from Bitcraze.

# A. Fabrication of the gripper

The bistable gripper is made up of 4 parts: the contact pad, tube, the fingers (upper and lower), and the base with beams. Besides the tube and revolute joint shafts, all the parts are 3D printed with Polylactic acid (PLA) using a Prusa i3 MK3 printer. The tube is made of silicone rubber (5054K304, McMaster-Carr) and has an inner diameter of 1 mm and outer diameter of 3 mm. The upper fingers are glued to the lower ones. Note that the upper finger can be designed separately with any dimensions or shapes (angles and lengths) to hold or carry objects with different sizes.

Using the design guideline, we choose the basic activation forces to be (0.8 N, -0.6 N). Then Eq. (6) are solved in Matlab using a built-in function "vpasolve" with other predefined parameters  $L_0=15.16$  mm,  $\alpha=0^\circ$  and  $\beta=30^\circ$ . Solutions of Eqs. (6) generate the ideal linear spring constant  $\bar{k}_d=590$  N/m and torsion constant  $\bar{k}_\theta=1.5\times10^{-3}$  Nm/rad. Then we use the following equation

$$k_d = \frac{3E_1I_1}{l_1^3}, \quad k_\theta = \frac{E_2I_2}{l_{tube}}$$
 (7)

to calculate the dimension of the beam, where  $I_1$ ,  $I_2$  is the second moment of the area,  $E_1$ ,  $E_2$  is the Young's modulus of the beam and tube, respectively. The detailed design parameters are shown in Table I. With the above parameters, the actual constants  $k_d = 526$  N/m and  $k_\theta = 1.2 \times 10^{-3}$  Nm/rad.

We fabricate three grippers to validate the modeling results: one base gripper  $(G_0)$  with  $\alpha=0$ ,  $G_1$  with  $\alpha=2.5^\circ$  and  $G_2$  with  $\alpha=5^\circ$ , of which the ideal activation forces( $\bar{F}_{max}$  and  $\bar{F}_{min}$ ) are (0.8 N, -0.6 N) and (1.33 N, -1.1 N), and (1.95 N, -1.72 N), respectively. We list some important parameters of the three grippers in Table II.

# B. Activation forces test experiment

The activation forces of the three grippers are measured to show the accuracy of the mathematical model and the performance of the design guideline.

TABLE I
DESIGN PARAMETERS FOR THE BISTABLE GRIPPER

Parameter	Dimension		
$l_1(mm)$	29		
$l_2(mm)$	15		
$\overline{l_{tube}(mm)}$	5		
$\overline{l_p(mm)}$	6.5		
$oldsymbol{eta}(^{\circ})$	30		
$h_b(mm)$	3		

TABLE II  $\alpha \text{ and activation forces for 3 different bistable gripper} \\$ 

Parameters	$G_0$	$G_1$	$G_2$
$lpha(^\circ)$	0	2.5	5
$\overline{F}_{max}(N)$	0.8	1.33	1.95
$ar{F}_{min}(N)$	-0.6	-1.1	-1.72
$\overline{F_{max}(N)}$	0.87	1.43	2.04
$\overline{F_{min}(N)}$	-0.56	-1.11	-1.75
$e_{max}(\%)$	8.5	7.52	4.62
$e_{min}(\%)$	6.7	0.9	1.74

The experiment setup is shown in Fig. 6. To test the activation force, we design a disk to stabilize the base to the tip of a linear actuator(FR-L12-100-210-6-I, Actuonix Motion Devices). With the disk, twisting motion of the tube can be avoided. The contact pad is glued to the tip of a force gauge (M3-5, Mark-10). The linear actuator is controlled to move back (for  $F_{max}$ ) or forward (for  $F_{min}$ ) with a constant speed of 2 mm/s. At the same time, the force is recorded. For each gripper, we conduct 3 experiments for both  $F_{max}$ and  $F_{min}$ . The mean activation forces and error for each gripper are listed in Table II. Absolute error  $e_{max}$  and  $e_{min}$ show the error for the corresponding activation forces. From the table, we can see that the proposed activation force estimation method is accurate especially when the absolute forces are large. It is because the moments caused by the tubes have much less influence than that from the bending beams when the beams are initially tilted. In addition, during the experiments, except bending, the tube is also deformed, which influences the results, especially when the force from bending beam is small.



Fig. 6. Activation forces test setup

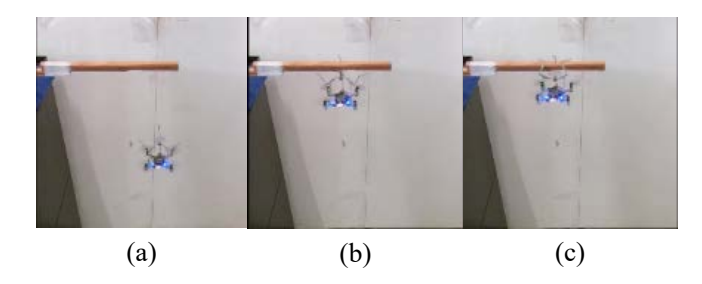


Fig. 7. Image sequence showing the perching process.

## C. Perching experiment with Crazyflie

With the modeling of force-displacement characteristics, a gripper with desired activation forces can be designed for different flying robots. However, since perching and carrying payload just defers from the installation of the gripper (top or bottom of a flying robot), we only test the perching capability in this paper. For the flying robot we use Carzyflie 2.0, which has a maximum thrust of 57 g with a weight of 27 g. With the bistable gripper and releasing device, the total weight of the system is 36 g, meaning an extra thrust of 21 g can be provided. Based on the weight of Crazyflie and its thrusts, we designed a gripper with  $F_{max} = 0.6$  N and  $F_{min} = -0.2$  N.

The whole perching system is shown in Fig. 1. The gripper is installed on top of the Crazyflie. A motor driver (DRV8838, Pololu) is used to apply voltage to the resistance wires. With currents going through the wires, the upper fingers made from PLA would be soften and release the Crazyflie. In the perching experiment, Crazyflie is controlled manually to elevate towards a wood rod. The gripper can be closed with the spare thrust. After changing state, the three upper fingers will close and hold the Crazyflie. Once the Crazyflie receives the taking off signal, it will enable the motor driver to apply current to the resistance wires. Once the temperature is higher than the glass transition temperature of the upper finger material (PLA), the upper finger will become soft and release the Crazyflie. After releasing, the motors are immediately turned off. The image sequence of the perching is shown in Fig. 7. The result shows the perching can be successfully achieved.

## V. CONCLUSIONS AND FUTURE WORK

In this paper, we investigate a miniature bistable gripper that can be used for perching of small flying robots. The gripper can achieve three requirements: easy to close, stable to hold, and easy to adjust. Mathematical models and the design guideline of the gripper are discussed. Based on the design guideline, we can achieve different activation forces for closing and opening by properly designing the gripper. Experiments are conducted to measure the activation forces for three grippers. Experimental results show that the developed mathematical model can predict the activation force precisely. Also, preliminary perching experiments with a palm-size quadcopter is conducted. Results show that the gripper can make the robot perch on a horizontally hanged object.

#### REFERENCES

- [1] D. Floreano and R. J. Wood, "Science, technology and the future of small autonomous drones," *Nature*, vol. 521, no. 7553, p. 460, 2015.
- [2] W. R. Roderick, M. R. Cutkosky, and D. Lentink, "Touchdown to take-off: at the interface of flight and surface locomotion," *Interface focus*, vol. 7, no. 1, p. 20160094, 2017.
- [3] M. Kovac, "Learning from nature how to land aerial robots," *Science*, vol. 352, no. 6288, pp. 895–896, 2016.
- [4] H. Zhang and J. Zhao, "Vision based surface slope estimation for unmanned aerial vehicle perching," in ASME 2017 Dynamic Systems and Control Conference, pp. V003T39A011–V003T39A011, American Society of Mechanical Engineers, 2018.
- [5] H. Zhang, B. Cheng, and J. Zhao, "Optimal trajectory generation for time-to-contact based aerial robotic perching," *Bioinspiration & biomimetics*, vol. 14, no. 1, p. 016008, 2018.
- [6] M. Graule, P. Chirarattananon, S. Fuller, N. Jafferis, K. Ma, M. Spenko, R. Kornbluh, and R. Wood, "Perching and takeoff of a robotic insect on overhangs using switchable electrostatic adhesion," *Science*, vol. 352, no. 6288, pp. 978–982, 2016.
- [7] M. Kovač, J. Germann, C. Hürzeler, R. Y. Siegwart, and D. Floreano, "A perching mechanism for micro aerial vehicles," *Journal of Micro-Nano Mechatronics*, vol. 5, no. 3-4, pp. 77–91, 2009.
- [8] D. Mehanovic, J. Bass, T. Courteau, D. Rancourt, and A. L. Desbiens, "Autonomous thrust-assisted perching of a fixed-wing uav on vertical surfaces," in *Conference on Biomimetic and Biohybrid Systems*, pp. 302–314, Springer, 2017.
- [9] J. Thomas, M. Pope, G. Loianno, E. W. Hawkes, M. A. Estrada, H. Jiang, M. R. Cutkosky, and V. Kumar, "Aggressive flight with quadrotors for perching on inclined surfaces," *Journal of Mechanisms* and Robotics, vol. 8, no. 5, p. 051007, 2016.
- [10] M. T. Pope, C. W. Kimes, H. Jiang, E. W. Hawkes, M. A. Estrada, C. F. Kerst, W. R. Roderick, A. K. Han, D. L. Christensen, and M. R. Cutkosky, "A multimodal robot for perching and climbing on vertical outdoor surfaces," *IEEE Transactions on Robotics*, vol. 33, no. 1, pp. 38–48, 2017.
- [11] C. E. Doyle, J. J. Bird, T. A. Isom, J. C. Kallman, D. F. Bareiss, D. J. Dunlop, R. J. King, J. J. Abbott, and M. A. Minor, "An avian-inspired passive mechanism for quadrotor perching," *IEEE/ASME Transactions on Mechatronics*, vol. 18, no. 2, pp. 506–517, 2013.
- [12] T. Schioler and S. Pellegrino, "Space frames with multiple stable configurations," AIAA journal, vol. 45, no. 7, pp. 1740–1747, 2007.
- [13] T.-A. Nguyen and D.-A. Wang, "A gripper based on a compliant bitable mechanism for gripping and active release of objects," in Manipulation, Automation and Robotics at Small Scales (MARSS), International Conference on, pp. 1–4, IEEE, 2016.
- [14] T. Chen, J. Mueller, and K. Shea, "Integrated design and simulation of tunable, multi-state structures fabricated monolithically with multimaterial 3d printing," *Scientific reports*, vol. 7, p. 45671, 2017.
- [15] T. Chen, O. R. Bilal, K. Shea, and C. Daraio, "Harnessing bistability for directional propulsion of soft, untethered robots," *Proceedings of the National Academy of Sciences*, p. 201800386, 2018.
- [16] A. Alqasimi, C. Lusk, and J. Chimento, "Design of a linear bistable compliant crank-slider mechanism," *Journal of Mechanisms and Robotics*, vol. 8, no. 5, p. 051009, 2016.
- [17] G. Li and G. Chen, "A function for characterizing complete kine-tostatic behaviors of compliant bistable mechanisms," *Mechanical Sciences*, vol. 5, no. 2, pp. 67–78, 2014.
- [18] J. Qiu, J. H. Lang, and A. H. Slocum, "A curved-beam bistable mechanism," *Journal of microelectromechanical systems*, vol. 13, no. 2, pp. 137–146, 2004.
- [19] N. Hu and R. Burgueño, "Buckling-induced smart applications: recent advances and trends," *Smart Materials and Structures*, vol. 24, no. 6, p. 063001, 2015.
- [20] J. Sun and J. Zhao, "An adaptive walking robot with reconfigurable mechanisms using shape morphing joints," *IEEE Robotics and Au*tomation Letters, vol. 4, pp. 724–731, April 2019.
- [21] R. Mises, "Über die stabilitätsprobleme der elastizitätstheorie," ZAMM-Journal of Applied Mathematics and Mechanics/Zeitschrift für Angewandte Mathematik und Mechanik, vol. 3, no. 6, pp. 406–422, 1923.
- [22] P. Kelly, "An introduction to solid mechanics," *Lecture notes*, pp. 229–270, 2013.